Effect of phyllosilicate type on the microstructure and properties of kaolin-based ceramic tape

Waltraud Kriven, Jingyang Wang, Yanchun Zhou, Dongming Zhu, Gustavo Costa, Manabu Fukushima, Andrew Gyekenyesi

EFFECT OF PHYLLOSILICATE TYPE ON THE MICROSTRUCTURE AND PROPERTIES OF KAOLIN-BASED CERAMIC TAPES

Gisèle L. Lecomte-Nana[*a], Khaoula Lebdioua[a,b], Mylène Laffort[a,c], Nadia Houta[a], Nicolas Tessier-Doyen[a], Younès Abouliatim[b], Claire Peyratout[aa]

Laboratoire Science des Procédés Céramiques et de Traitements et Surface (SPCTS), UMR CNRS 7315, CEC - ENSCI, 12 rue Atlantis, 87068 Limoges Cedex, France[b] Laboratoire Matériaux Procédés Environnement Qualité, LMPEQ, Université Cadi Ayyad - Ecole Nationale des Sciences Appliqués de Safi, Route Sidi Bouzid, BP 63 - 46000 Safi, Maroc[c] Institut de Chimie des Milieux et Matériaux de Poitiers (IC2MP), UMR 7285 CNRS - Université de Poitiers – SFA, 4, rue Michel Brunet (Bât B27), TSA 51106, 86073 Poitiers cedex 9 France

ABSTRACT

The purpose of this work was to highlight the effective influence of the nature and shape of clay minerals on the texture, sintering behavior and the final characteristics of kaolin-based ceramics shaped by tape casting. Palygorskite (P) and talc (T), which are respectively 2:1 and fibrous-like clay minerals, were added into aqueous slurries of kaolin in various amounts: 10, 20, 30, 40, and 50 mass % (with respect to kaolin + added clay). The clay materials and different tapes (consolidated as well as green tapes) were characterized using chemical, structure, microstructure, and thermal analyses together with flexural bi-axial tests.

The increase of talc content into kaolin-based slurries from 10 to 50 mass % did not significantly affect the rheological behavior according to the tape casting process. For palygorskite, the binder and plasticizer content were modified accordingly. Both kaolin-P and kaolin-T tapes exhibited a highly textured microstructure within the thickness. Nevertheless, the increasing amount of the palygorskite content up to 20 mass% tended to significantly decrease the open porosity while preserving the difference in roughness between the top and bottom surfaces of the tapes sintered at 1100°C. With talc, 10 mass% appeared as a threshold content above which the addition of talc was detrimental both for the porosity and the flexural bi-axial strength. The optimal properties of use were obtained for the tapes containing 50 mass% of talc (sintering at 900°C); 20 mass% of palygorskite or 10 mass% of talc (sintering at 1100°C).

I.INTRODUCTION

From the 1940s, ceramic or metal layers shaped by tape-casting have focused on the development of filtration membranes, fuel cells or multilayer ceramic capacitors. This shaping process presents the advantage of organizing microstructures of powder compacts by addition of anisotropic grains to manufacture laminated tapes with a regular surface, thickness, microstructure and density. Processes such as centrifugation, pressing extrusion are extensively used in a wide range of ceramic materials: clay, alumina, silica and many other minerals. Contrary to these processes, tape-casting is more dedicated to the production of thin substrates whose typical thickness is from 25 µm and 1600 µm, or multilayer structures.

A great interest is directed to clay-based materials whereby the chemical and physical interactions are investigated. Clay minerals are the most important chemical weathering product of the soil defined as those finely divided crystalline aluminosilicates which belong to the

* Corresponding Author

phyllosilicates family. More specifically, kaolin, palygorskite and talc are natural occurring rocks mainly composed of kaolinite, palygorskite and talc minerals respectively. In general talc is mainly associated with chlorites and other secondary faces. In order to clarify the specificity of these clays, the description of the related clay minerals (kaolinite, talc and palygorskite) are developed below. Kaolinite and talc are both phyllosilicates minerals (a subgroup of the silica), their main characteristic is the layer structure, while palygorskite offers a fibrous-like shape due to the regular mis-stacking of subsequent layers.[1,2]

Kaolinite is a 1:1 or TO (tetra:octa) layer type with an inter-reticular distance of 7.1Å. It is a dioctahedral alumino-silicate with the chemical formula: $Si_2O_5Al_2(OH)_4$, considered to be hydrophilic.[3] It has an important role because of its high abundance in nature, relatively pure chemical composition, and well characterized crystal structure[4,5]. This structure is characterized by a unit cell composed of an aluminous di-octahedral sheet coordinate to a layer of silicon tetrahedral sheet (Figure 1(a)). Kaolinite lamellae have negatively charged sites owing to the substitution of the central Si- and Al-ions in the crystal lattice for lower positive valence ions. Kaolinite particles consist of about 50 silicate layers which are held together by hydrogen bonds and Van der Waals interactions. The major transformations of kaolinite during heating are dehydroxylation between 450-650°C and a structure reorganization around 950°C (whereby the crystallization of mullite is initiated, of formula: $3Al_2O_3.2SiO_2$) [6]. Halloysite has a structure very similar to that of kaolinite. The main difference is the shape of halloysite particles that can be platelet-like or tube-like depending on the pH value of the medium.

Talc is a 2:1 layer type, with an inter-reticular distance of 9.35Å. It's a trioctahedral magnesium-silicate with the chemical formula: $Si_4O_{10}Mg_3(OH)_2$, considered hydrophobic (its dispersion in water is complex). The unit layer structure (Figure 1(b)) is to be composed of three magnesium octahedra per four silicon-based tetrahedra. [3] In general the dehydroxylation in the range of 100°C mass loss of 4% and the crystallization of high faces (clinoenstatite, of formula: $MgO.SiO_2$) arises above 800°C[6].

Palygorskite (also known as attapulgite) is from phyllosilicate family of clay minerals and contains a continuous two-dimensional tetrahedral sheet with a fibrous habit. However, it differs from other layer silicates in that they lack continuous octahedral sheets. The structure of palygorskite (Figure 1(c)) contains ribbons of 2:1 (TOT) layer-type phyllosilicates linked by periodic inversion of the apical oxygen of the continuous tetrahedral sheet for every four atoms of Si (two tetrahedral chains). Ribbons extend parallel to the axis of the fiber). In this framework, rectangular channels run parallel to the X-axis between opposing 2:1 ribbons. The tetrahedral sheet is continuous across ribbons but the octahedral sheet is discontinuous as a result of the periodic inversion, and terminal octahedral cations must complete their coordination sphere with water molecules referred to as coordinated water. According to the structure proposed by Bradley 1940[7] palygorskite has five possible octahedral positions per its half unit cell with ideal formula of $Si_8Mg_5O_{20}(OH)_2(OH)_4.H_2O$ where OH_2 denotes bound water and H_2O represents water held in channels (Callière and Hénin 1961b.). Although the five positions cannot be filled[8], a dioctahedral mineral with a structural formula $Si_8O_{20}Al_2Mg_2(OH)_2(OH_2)_4 \cdot 4H_2O$ is accepted. The presence of micropores and channels in these minerals, together with the fine particle size and fibrous habit, account for their high specific surface area.

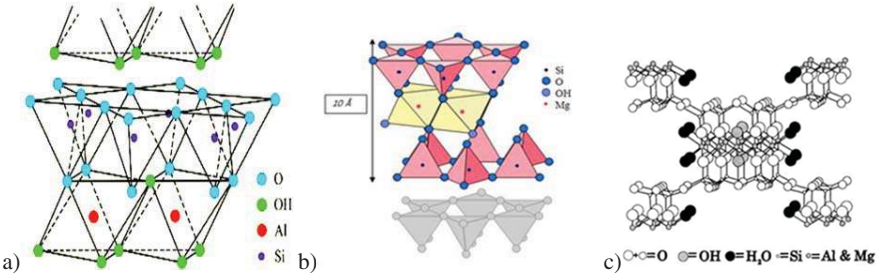

Figure 1. Typical structure of (a) kaolinite, (b) talc and (c) palygorskite minerals

Recently, it was shown that a thermal treatment higher than 1100°C of a kaolinite-based layered material induces the growth of mullite crystals which tends to improve mechanical properties of a highly organized network[9,10]. Mechanical properties of individual tapes can be significantly increased by introducing a slight proportion of long aluminosilicate fibers. The purpose of this work was to highlight the effective influence of the nature and shape of clay minerals on the texture, sintering behavior and the final characteristics of kaolin-based ceramics tapes. Palygorskite (P) and talc (T), were added into aqueous slurries of kaolin in various amounts: from 10 to 50 mass %.

MATERIALS

The three raw materials that have been studied are: BIP Kaolin (major constituent is kaolinite, $Al_2SiO_5(OH)_4$) provided by Kaolin de Beauvoir, France, a fiber-like clay palygorskite (2:1 type clay, $Si_8O_{20}Al_2Mg_2(OH)_2(OH_2)_4 \cdot 4H_2O$) supplied by Hangzhou Dayanchem Co. LTD, China, and the talc (2:1 type clay, $Si_4O_{10}Mg_3(OH)_2$) gratefully provided by Imerys, Limoges, France, were characterized prior to their use. The chemical compositions of these clays were obtained from their technical data sheets and are listed in Table 1. Kaolin, talc and palygorskite are denoted in this study as K, T and P.

Table 1. Chemical compositions (wt.%) of the different clays

	SiO_2	Al_2O_3	K_2O	Na_2O	MgO	CaO	Fe_2O_3	TiO_2	Li_2O	Loss on ignition
Kaolin	48.1	39.9	1.9	<0.2	0.17	<0.2	0.26	<0.25	0.27	10
Talc	63	0.2	0.01	0.03	30.5	0.25	1.4	<0.1		4.7
Palygorskite	55.3	10.24	0.47	-	10.49	-	3.53	-	-	20

III. METHODS

III.1. Tape casting process

Tape casting is a well-known shaping process commonly used in the field of ceramics. It consists of spreading a liquid suspension (slurry) on to a fixed support composed of a flat glass

substrate coated with a Mylar film (Figure 2). The suspension is stored in a sliding container. The relative motion between the container and the glass substrate allows the spreading of the suspension. A blade laminates the suspension and determines the thickness of the green suspension. [9] A shear-thinning rheological behavior is necessary to favor the even spreading of the suspension while avoiding sedimentation of particles. Moreover, theviscosity value at a specific shear-rate (10 s^{-1}) has to range between 0.6 and 1 Pa.s to favor the proper spreading of the suspension.

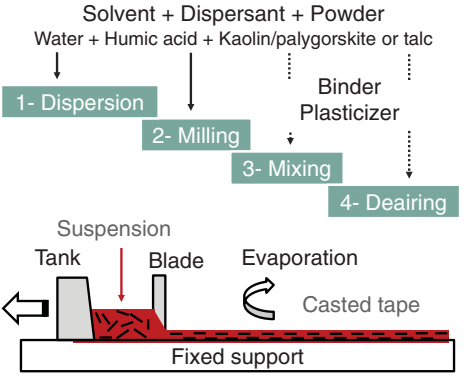

Figure 2: Simplified representation of a tape casting set-up and slurry preparation

A typical tape casting slurry contains the required powder, a solvent (aqueous or organic) and specific additives in appropriate amount. These additives are namely:

- A deflocculant, that helps in dispersing the solid particles within the solvent
- A binder, that improves the cohesion of green tapes
- A plasticizer, that promotes the flexibility of green tapes upon handling

In literature the key parameter of well dispersed slurries for tape casting is the ratio between binder/plasticizer, generally in the range of 0.5 to 1 by weight.

In terms of additives Dolaflux® (a biopolymer), polyvinyl alcohol (PVA 2200) and polyethylene glycol (PEG) are used as deflocculant, binder and plasticizer respectively. A binder/plasticizer ratio (by weight) of 1 was used to formulate the different slurries.

III.2. Slurry Preparation

The 0.1 $g.mL^{-1}$ dispersant solution was prepared by dissolving Dolaflux® in a 3M NaOH solution. Aqueous suspensions were prepared using deionized water and a constant clay proportion of 62.5 mass %. One suspension, containing only kaolin is noted K_{100}(T or P)$_0$ whereas another one, noted $K_{90}H_{10}$, is composed of 90 mass% of kaolin and 10 mass% of halloysite. Suspensions were prepared with 0.1, 0.2 and 0.3 mass % of dispersant with respect to the clay content. Prior to further measurements, suspensions were mixed using a roll mixer for 24 h at room temperature in order to promote interactions between the clay particles and additives while removing residual air bubbles.

Previously dispersed clay suspensions were milled in a planetary mill during 6 h at 180

rpm to break up the coarser agglomerates. Then, the binder and the plasticizer were introduced, the ratio binder/plasticizer being equal to 1 by weignt. The binder content was kept constant to 5 mass% with respect to the clay content. The 0.16 $g.mL^{-1}$ binder solution was prepared by incorporating PVA slowly in deionized water which was previously heated at 80°C. During addition of PVA, the solution was constantly stirred in order to avoid the formation of a gel. Slurries were then mixed in the planetary mill during 15 h at 100 rpm to prevent the breaking of organic molecules. The suspension was then de-aired for 10 h on a roll mixer at 32 rpm and then during 15 h on a roll mixer at 4 rpm. Slurries were then sieved at 100 µm to ensure the elimination of the non-dissolved binder or impurities related to the milling step. A rheological characterization was conducted to check the shear-thinning behavior and viscosity value at 10 s^{-1}. The nomenclature adopted for suspensions was $K_{100-x}(T \text{ or } P)_x$ where K, T and P correspond to kaolin, talc and palygorskite respectively; x was the amount of talc or palygorskite in mass% with respect to the clay content.

III.3. Characterization Techniques

III.3.1. Morphology, Structure And Microstructure

X-ray diffraction measurement was carried out on raw powders with a Bruker D5000 X-ray powder diffractometer equipped with a crystal monochromator employing Cu-Kα radiation of wavelength 1.5406 Å at room temperature. The measurements were performed at 40 kV and 30 mA in a 2θ range from 2° to 70°, with a 2θ scanning rate of 0.5 °/min and a step of 0.02°.

Scanning electron microscope (SEM) observations (Stereosacan Cambridge S260 SEM microscope) were performed on bottom and upper faces as well as on sides of tapes. To prepare samples, upper and bottom faces of specimens are set on carbon adhesive patches to stick to the sample holder. Fractures of tapes were set vertically on carbon paste to observe slices. Silver lacquer was evently applied on samples surfaces. In all cases, a 15 mm gold layer was deposited in order to improve the electrical conduction at the surface of samples (to improve the quality of the images).

III.3.2. Physical Properties

The laser diffraction technique was use to measure the particle size distributions. The grain size distribution was obtained with a “Mastersizer 2000” device through the liquid route. For each sample the analysis was repeated at least 3 times, and an average value was given. Three different methods were used to determine the specific density, apparent density and open porosity of the studied samples.

For the powdered specimens an helium pycnometer was used. The method consisted in putting a known mass of the previously dried powder into a cell of known volume. The difference between the cell volume and the helium volume that was needed to fill corresponds to the effective volume of the solid powder. The latter measurement allows calculating the specific density of the powder.

The bulk density and open porosity of the sintered pellets wre measured by the vacuum method. This method is suiTable for determining open porosity values higher than 1% and for an average pore size lower than 200µm. The mass of the sample was measured under three different conditions: i) completely dry, ii) impregnated by water under vacuum and immersed into water, and iii) impregnated by water under vacuum and weight in ambient air.

The volume of unfired pellets was measured by a less precise method. Their volumes

were determined by the measurement of the diameter and the thickness of the pellets, and their masses were weighed. The ratio mass/volume gave the apparent density of the pellets.

III.3.3. Thermal Analyses

Differential thermal and gravimetric analyses (DTA/DTG) were carried out on the phyllosilicate powders in the temperature range 25 °C – 1300 °C at a heating rate of 5°C/min under dried-air atmosphere using a SETSYS 2400 DTA-TGA equipment from SETARAM. Prior to analysis, the samples were oven-dried at 100°C for at least one day or until constant weight was achieved. Alumina powder, previously calcined at 1500 °C for 1 h, was used as a reference material. All analyses were performed using 50 mg aliquots of sample and reference.

Dilatometric analyses were performed using a horizontal Netsch 202 C which detected in situ the length variation of samples in the same conditions as for DTA-TGA analyses. The thermal behavior heled to determine the most appropriate thermal cycle during sintering in order to avoid cracks formation within sintered products.

III.3.4. Rheology

Rheological measurements were performed at 25°C using a parallel-plate geometry (lower Peltier plate; upper plate with 40 mm in diameter) measured on a stress-controlled rheometer AR 1500ex from TA Instruments. The flow curve (upward) was measured with a shear stress ramp over 1 min from 0 to 15 Pa. A stabilization step was applied at 15 Pa for 30 s before performing a reversed ramp to measure the downward flow curve. The general behaviour was modelled using the Herschel-Bulkley equation (equation (1)):

$$\tau = \tau_0 + k\dot{\gamma}^n \quad (1)$$

with, τ_0: shear stress (Pa)

K: consistency (Pa.s)

$\dot{\gamma}$: shear rate (s^{-1})

n: flow index

To verify the good viscosity of the slurry the shear rate is calculated with the following formula (relation (2)

$$\dot{\gamma} = \frac{v}{e} \quad (2)$$

v = casting speed (cm/s) = 1cm/s; e = cast thickness (cm) = 10^{-1}cm;

thus $\dot{\gamma}$:= v/e = $10s^{-1}$.

III.3.5. Properties of use

Biaxial bending tests were carried out using a universal testing machine “Lloyd Easy Test EZ 20” driven by NEXIGEN PLUS 3.0 software equipped with a piston-ring configuration. The crosshead velocity and the preload were fixed at 0.5 $mm.min^{-1}$, 0.2 N respectively. A high sensitivity sensor (100 N) has been chosen because load submitted to specimens has to represent at least 1% of the maximum range. Samples used for biaxial bending tests were shaped in 30

mm in diameter disks. Experimental procedure has been applied in agreement with the standard method recommended for a piston on 3 balls configuration (ASTM Standard F394-78). The exact theoretical expression of the ultimate tensile strength at the center of the lower face is given by Glandus[11] according to the analytical calculations proposed by Kirstein and Wooley [12] (equation 3).

$$\sigma_R = \frac{3P_R(1+\nu)}{4\pi e^2}\left(1 + 2 * \ln\left(\frac{A}{B}\right) + \left(\frac{1-\nu}{1+\nu}\right) * \left(1 - \frac{B^2}{2A^2}\right)\frac{A^2}{C^2}\right) \qquad (3)$$

In this formula, geometrical parameters concerning the configuration (A: diameter of the ring equal to 28 mm and B: diameter of the upper piston equal to 5 mm) are required to calculate maximum stress to rupture □R. For all tested specimens, thickness (e) and diameter (C) have been voluntarily imposed (0.33 mm and 30 mm respectively) to avoid possible significant differences in stress values attributed to different volume under constraint. P_R corresponds to the ultimate load value at catastrophic fracture (N) and υ is the Poisson's ratio.

IV. RESULTS AND DISCUSSION

IV.1. Characterization of initial clay materials

Prior to their utilization, the major and secondary phases of starting clays were determined using XRD (Figures are not shown here). For the kaolin sample, the main constituent was kaolinite as expected, associated with quartz and muscovite as secondary phases. While the talc sample exhibited mainly the characteristic peaks of talc and very low signal corresponding to chlorites. In the case of palygorskite, the predominant crystalline phase was palygorskite with quartz as an accessory phase.

The characterizations of the talc powder using thermal analyses (DTA-TG) are presented in Figure 3. The first peak endothermic ① was due to the dehydration of the powder from the beginning to approximatively 70°C, with a very small mass loss. The second endothermic peak ② was related to the dehydroxylation of the talc from 800 to 950°C, with a mass loss close to 3.5%.

The characteristic particle sizes of kaolin, talc and palygorskite are provided in Table 2. Concerning kaolin particles, 50% of the particles detected by the laser diffraction granulometer were below 7.54 ⊠m while it was below 10.70 ⊠m for talc. Palygorskite appeared as the clay containing finer particles. One reason explaining this trend was the aggregation of the clay particles. Also the shape of these particles may have influenced the final results, depending on the effective interaction with the laser during the measurement. The specific densities of these clays were quite similar (close to 2.6 g/cm^3) while palygorskite exhibited the highest specific surface area. The latter observation was in agreement with the structure of palygorskite whereby inner channels were present and therefore may have contributed to increase the available surface of each particle.

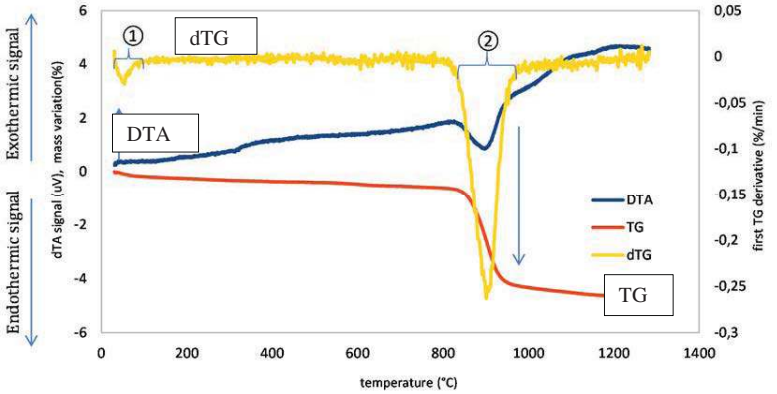

Figure 3. Thermal analysis diagrams of the starting talc clay

Table 2. Characteristic sizes and other physical parameters of kaolin, talc and palygorskite

Sample	D_{10} (µm)	D_{50} (µm)	D_{90} (µm)	BET Specific surface area (m^2/g)	Specific density (g/cm^3)
Kaolin **(K)**	2.46	7.54	32.92	11.7	2.6
Talc **(T)**	3.10	10.70	40.10	11.0	2.7
Palygorskite **(P)**	0.23	3.50	18.43	134.0	2.6

IV.2.Characterization of the kaolin-based tapes

IV.2.1. Kaolin-Palygorskite

The various tapes elaborated using palygorskite and kaolin were successfully recovered after drying without cracking. The thermal analyses that were performed on theses samples are illustrated in Figure 4. The typical DTA-TG curves (Figure 4(a)) showed two main regions associated with a great mass loss, namely between 200°C and 400°C and between 450°C and 780°C. The heating and cooling rates were determined using thermogravimetric and differential thermal analyses. From 250°C to 780°C, a high weight loss (14.5 %) occurred due to the degradation of organics and the dehydroxylation of clay minerals, implying that the heating rate had to be reduced to avoid cracking of samples.

The detailed phenomena that were denoted on the thermodilatometry curve (Figure 4(b)) were:

i)-from 30°C to 150°C due to the evaporation of free water,

ii)-from 800°C to 1000°C in relation with structural reorganization and

iii)-from 1050°C to 1400°C due to densification.

Based on these results, three temperature values of sintering (850°C, 1000°C and 1200°C) were chosen to understand the influence of the microstructural state on the stress to rupture values.

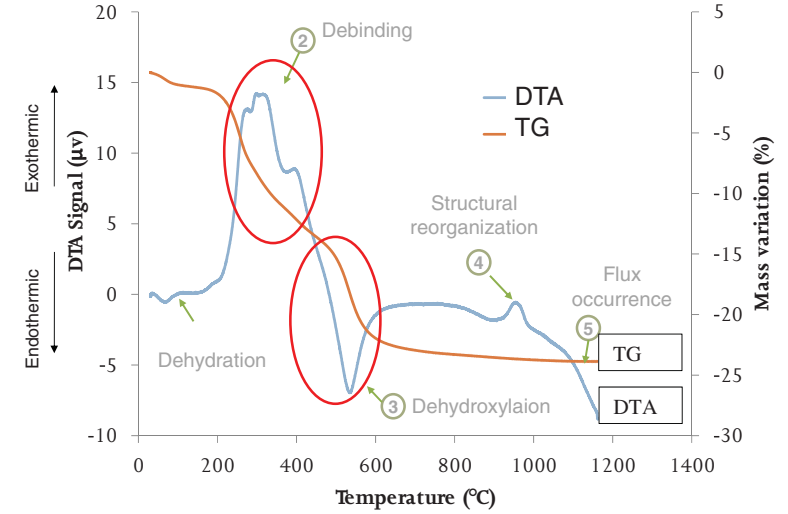

a)

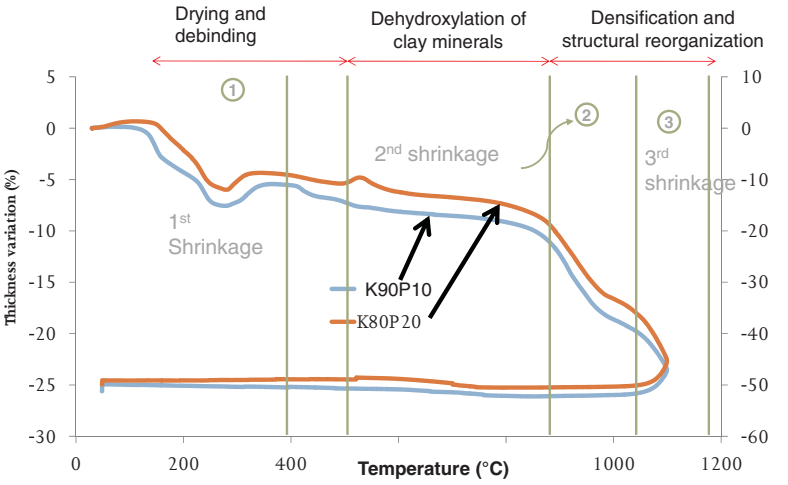

b)

Figure 4. Thermal analysis curves of typical kaolin-palygorskite tapes a) DTA-TG and b) thermodilatometry. Heating rate = 5°C/min under dry air

The results of the mechanical stress of rupture (σ_R) for some samples before and after sintering at 1100°C are presented on Figure 5. Regardless of the initial tape thickness, the presence of palygorskite tended to increase the stress of rupture of green tapes for at least 40%. While changing the thickness from 1 mm to 1.6 mm, the increase of palygorskite content from 10 to 20 mass % seemed to be detrimental for the green tape mechanical strength.

Upon sintering at 1100°C, the stresses of rupture of palygorskite containing tapes are significantly decreased while those for K100P0 tapes are increased. To justify these trends, it can be assumed that for the green tapes, the palygorskite needle-like particles and their characteristic channels helped to improve the plasticity of the related tapes and also acted as cracks deflectors. Since during sintering, the internal structure of the starting palygorskite was strongly modified, the microstructure was deeply affected and may explain the decrease observed.

To highlight the mechanical behavior of the studied tapes, the correlation has been performed with the SEM observations and open porosity values. Figure 6 presents the obtained images that also highlight the orientation of particles induced by the shaping process. Slices and surfaces of green and sintered laminates materials are shown.

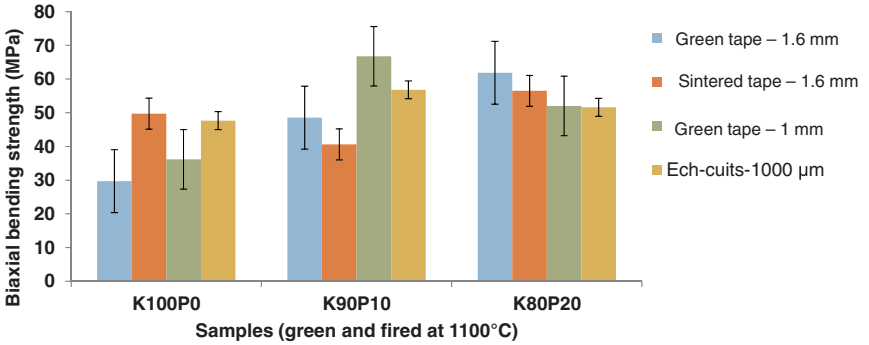

Figure 5. Biaxial flexural strength of some green and sintered (1100°C) kaolin-palygorskite samples. For each series from left to right: green tape 1.6 mm; sintered tape 1.6 mm; green tape 1 mmm and sintered tape 1 mm

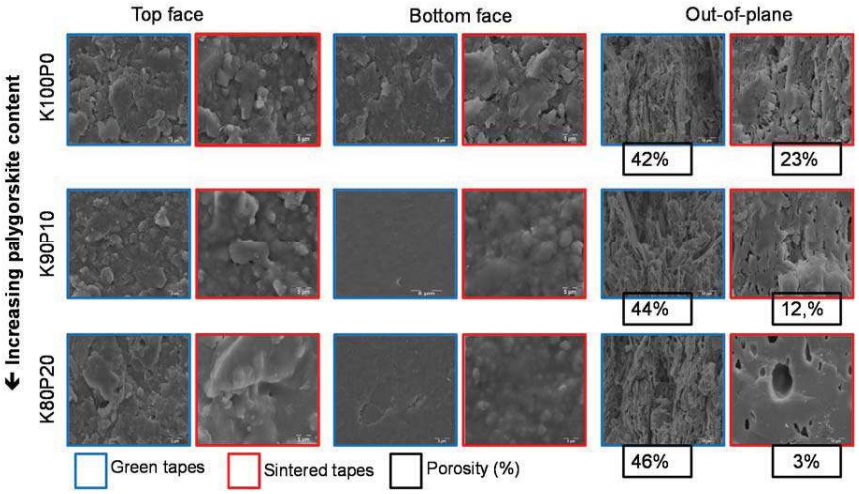

Figure 6. SEM micrographs and open porosity values of the kaolin-palygorskite samples before and after firing at 1100°C

For instance it appears that:

σ_R $K_{90}P_{10}$-1100°C (12%) < σ_R $K_{100}P_0$-1100°C (23%)

σ_R $K_{80}P_{20}$-1100°C (3%) > σ_R $K_{100}P_0$-1100°C (23%)

⇩ This result implies that the pore volume fraction is not the only parameter influencing stress to rupture values. It is possible that the pores size distribution and shape also contributed significantly as well as their connectivity. Furthermore, the microstructures of green tapes clearly showed a textured organization within the tapes. The latter was highly attenuated after sintering at 1100°C, due to the amorphization and the crystallization of high temperature phases (thermal transformations and interactions). Further experiments are needed to be performed at this stage to understand and clearly assess the predominant parameters that control the properties of use.

IV.2.2. Kaolin-Talc

In the case of kaolin-talc tapes, the DTA-TG analyses allow identification of the major transformations and the regions associated with important mass loss that should be considered for defining the firing cycle. Figure 7 illustrates the DTA-TG diagrams for the K50T50 sample, where the mains transformations are:

① = Dehydration of the powder, mass loss < 1%

② + ③ = Degradation of the organic compound with a weight loss of 8%

④ = Dehydroxylation of kaolinite associated to a mass loss of 4%

⑤ = Dehydroxylation of Talc, mass loss of 1.5%. and for the structural reorganization of metakaolinite.

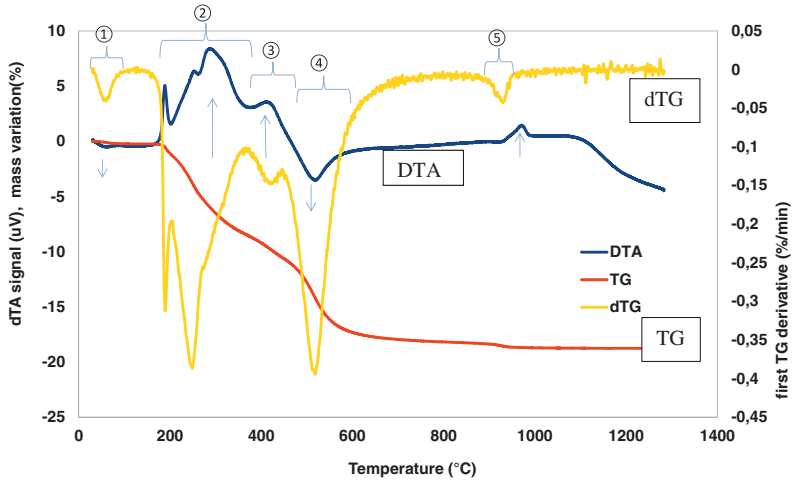

Figure 7. DTA-TG and DTG curves for the K50T50 sample (heating rate = 5°C/min, dry air)

According to the thermal analyses, three temperatures were also chosen to sinter the kaolin-talc samples: 900°C, 1000°C and 1100°C. The porosity and stress to rupture values obtained for various samples are presented in Figure 8. The mains observations can be summarized as follow:

- Green bodies:

All samples exhibited open porosity values between 44 and 50% regardless of talc content.
σ_R= 28 MPa, 32 MPa and 7 MPa were measured for respectively $K_{100}T_0$, $K_{90}T_{10}$ and $K_{50}T_{50}$ because of the difference in plasticity of both clays (talc is less plastic and less hydrophylic than kaolin).

- 900°C: σ_R= 8 MPa and 20 MPa were measured for respectively $K_{90}T_{10}$ and $K_{50}T_{50}$; related to the structural modification of metakaolinite.
- 1100°C: σ_R= 45 MPa, 50 MPa and 20 MPa for respectively $K_{100}T_0$, $K_{90}T_{10}$ and $K_{50}T_{50}$. Threshold talc content = 10 mass % to promote early sintering and preservation of mechanical properties.

Again the pore volume fraction variations do not justify such evolution of the mechanical properties. The contributions of the amorphous and crystalline phases are also preponderant.

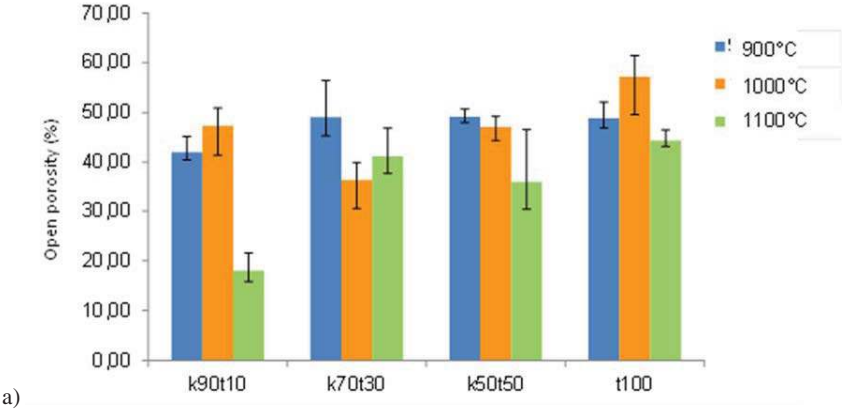

a)

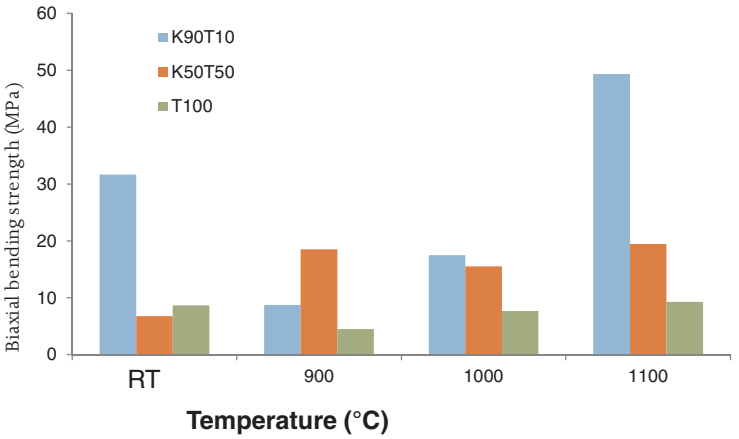

b)

Figure 8. a) Open porosity (from left to right: 900, 1000 and 1100°C) and b) stress to rupture values for some kaolin-talc tapes upon firing (from left to right: K90T10, K50T50 and T100)

V. CONCLUSION AND PROSPECTS

The present work aimed at understanding the influence of the type and morphology of clay minerals on the thermal behavior, microstructure and properties of use of kaolin-based ceramic tapes. The kaolin was substituted by either talc or palygorskite in proportions ranging from 0 to 50 mass % at least. (i) The clay characterizations allowed the verification oftheir mineralogical and chemical compositions that were in line with the expected results. Namely kaolin, talc and palygorskite contain kaolinite, talc and palygorskite as major crystalline phases. (ii) The thermal analyses (DTA, TG and dilatometry) that were performed on the studied tapes allowed the identification the critical high mass variation domains, in relation with the debinding/degradation of organics and dehydroxylation of clay minerals. The firing cycle have

been designed in correlation with these observations, and three firing temperatures were selected for each set of samples. (iii) The presence of palygorskite promoted the strengthening of green tapes, more than talc in relation with particle shape effects upon sintering both clays act as fluxing agents. (iv) When fired at 1100°C, the increase of talc content was detrimental since the stress to rupture were decreased, while with palygorskite, the level of mechanical strength was higher or close to that of sintered kaolin tapes. (v) The related trends were not completely justified by the pore volume fraction, thus the requirements existed for additional pores size distribution, shape and connectivity determination as well as the nature and amount of amorphous and crystalline phases in sintered samples.

ACKNOWLEDGEMENT

The authors are grateful to Gilles GASGNIER from Imerys Ceramic Centre located at Limoges, France for clays supply. The authors gratefully acknowledge the CARMALIM measurement center for offering facilities (SPCTS - ENSCI) at Limoges.

REFERENCES

[1] Dixon B., Schulze D. G., & Schulze D. G. (2002) « An Introduction to Soil Mineralogy », in *SSSA Book Series*, Soil Science Society of America.

[2] Bailey S.W. (1980) Structures of layer silicates. in: Crystal Structures of Clay Minerals and their X-ray Identification (G.W. Brindley& G. Brown, editors). Monograph 5, Mineralogical Society, London, pp. 1-123.

[3] Meunier A., Brief Digest For Clay Crystal Structure, available on : http://isterre.fr/spip.php?action=acceder_document&document&arg=1589&cle=eddfbf32086585e6bffe8aebbb6ab56ccb3bcac0&file=pdf%2FIMACS_UE1_Meunier_Clay_Mineralogy_Digest.pdf.

[4] Adams, J.M. (1983) Hydrogen-atom positions in kaolinite by neutron profile refinement. Clays and Clay Minerals, vol. 31, n°5, 352–356.

[5] Young, R.A., Hewat, A.W. (1988) Verification of the triclinic crystal-structure of kaolinite. Clays and Clay Minerals, vol. 36, n°3, 225–232.

[6] Jouenne C.A. (1990) *Traité de céramiques et matériaux minéraux*, p.244.

[7] . Bradley, W.F. (1940) The structural scheme of attapulgite. *American Mineralogist*, n°25, 405–411, GeoRefWeb of Science.

[8] Serna, C., Rautureau, M., Prost, R., Tchoubar, C., and Serratosa, J.M. (1977) Etude de la sépiolite a l'aide des données d ela micrsocopie électroniqe, de l'analyse thermo-pondérale et de la spectroscopie infrarouge. *Bulletin Groupe Française de Argiles*, XXVI, 153–163.

[9] Boussois K., Deniel S., Tessier-Doyen N., Chateigner D., Dublanche-Tixier C., & Blanchart P. (2013) "Characterization of textured ceramics containing mullite from phyllosilicates," *Ceram. Int.*, vol. 39, n°. 5, pp. 5327–5333,.

[10] Lecomte-Nana G., Mokrani A., Tessier-Doyen N., Boussois K., & Goure-Doubi H. (2013) "Texturation of model clay materials using tape casting and freezing," *Ceram. Int.*, vol. 39, n°. 8, pp. 9047–9053.

[11] Glandus J. C. (1986) "Meaning of the biaxial flexure tests of discs for strength measurements," *Le J. Phys. Colloq.*, vol. 47, n°. C1, pp. C1–595–C1–600

[12] Kirstein A. F. & Woolley R. M. (1967) "Symmetrical bending of thin circular elastic plates on equally spaced point supports," *J. Res. Natl. Bur. Stand. Sect. C Eng. Instrum.*, vol. 71C, n°. 1, p. 1.